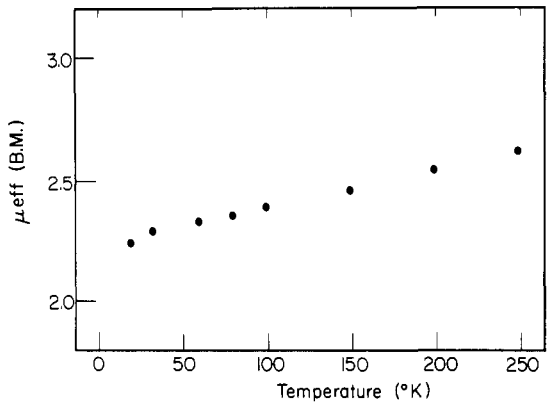

Figure 8. Plot of effective magnetic moment per iron ion (μ_{eff}) vs. temperature for dioxidized compound **5**.

lence-localized mixed-valence biferrocene. The two $S = {}^1/_2$ Fe^{III} ions in the dication of **5** must be involved in a magnetic exchange interaction that gives $S = 0$ and $S = 1$ states for the binuclear dication. The EPR signal arises from complexes that are in the $S = 1$ state. Two $\Delta M_s = \pm 1$ EPR transitions would be observed for each of the two principal components of the **g** tensor. Thus, the $g_\perp$ and $g_\parallel$ signals seen for an Fe^{III} ion (such as seen in Figure 5) each would be split into two signals by zero-field splitting. The zero-field splitting could result from either a through-space interaction of the two magnetic dipoles, one located at each Fe^{III} ion, or a pseudodipolar interaction. In the latter case, the $S = 1$ state is split by a spin-orbit interaction with an excited state. It is unfortunately not an easy matter to analyze the spectrum shown in Figure 7 for two reasons. First, since the spectrum encompasses such a large magnetic field range, including a portion of it very near zero field, it is difficult to simulate by the eigenfield method. Second, as seen for **2**, the two Fe^{III} metallocene moieties in **5** would be expected to be twisted relative to each other. The **g** tensors at the two Fe^{III} ions would most likely be misaligned. Single-crystal EPR data would be needed to interpret the EPR spectrum of **5**.

Magnetic susceptibility data were collected for **5** from 250 to 5.8 K. Figure 8 shows a plot of μ_{eff} per iron atom vs. temperature. As can be seen, μ_{eff}/Fe varies from 2.67 to 2.20 μ_B. There is no sign of an appreciable magnetic exchange interaction between the two $S = {}^1/_2$ ions in the dication of **5**. This is interesting since the Fe···Fe distance is ~4.6 Å and the unpaired-electron-containing $d_{x^2-y^2}/d_{xy}$ orbitals at each iron ion are directed from one iron toward the other iron ion. The exchange interaction that is indicated by the EPR results must be of such a magnitude that $|J|$ is less than ~0.5 cm^{-1}, where J is the exchange parameter in the spin Hamiltonian $\hat{H} = -2J\hat{S}_1\cdot\hat{S}_2$.

An IR spectrum for a KBr pellet of **5** is available in the supplementary material. It is important to note that there is a strong C-H bending band at 847 cm^{-1}. This is a value that is appropriate for an Fe^{III} metallocene.

Conclusions and Comments

The X-ray structure of **2** indicates a valence-localized structure for the mixed-valence *exo,exo*-1,12-dimethyl[1.1]ferrocenophane cation. Mössbauer, EPR, magnetic susceptibility, and IR data are in agreement with the structural results.

The dioxidized compound **5** has two $S = {}^1/_2$ Fe^{III} ions that are involved in a very weak intramolecular magnetic exchange interaction where the exchange parameter $|J|$ is less than ~0.5 cm^{-1}. It is curious that the $DDQH^-$ (monoanion of hydroquinone of 2,3-dicyano-5,6-dichloro-*p*-benzoquinone) salt of the dication in **5** has previously been reported[3] to possess a strong antiferromagnetic exchange interaction. It is possible that the dication in the $DDQH^-$ salt was the carbocation where both of the positive charges reside on the two bridging carbon atoms.

Acknowledgment. We are grateful for support from National Institutes of Health Grant HL13652 (D.N.H.).

Supplementary Material Available: Tables V-VII, listing structure factors and thermal parameters for compound **2** and IR data for *exo,exo*-1,12-dimethyl[1.1]ferrocenophane and for compounds **2** and **5**, and Figures 9-11, including plots of ln (area) of Mössbauer spectra vs. temperature for **2**, **5**, and ferrocenium triiodide, a plot of μ_{eff} vs. temperature for **2**, and a 400-1500-cm^{-1} IR spectrum of a KBr pellet of **5** (17 pages). Ordering information is given on any current masthead page.

Contribution from the Department of Chemistry, Purdue University, West Lafayette, Indiana 47907

Use of Spin-Magnetization-Transfer Techniques To Probe the Dynamic Behavior of (Dialkylamido)dimolybdenum Complexes

Timothy W. Coffindaffer, William M. Westler, and Ian P. Rothwell*

Received February 15, 1985

Addition of 2,6-diphenylphenol (HOAr) to the dinuclear compound $Mo_2(NMe_2)_6$ results in the formation of 1,2-$Mo_2(OAr)_2(NMe_2)_4$ when hexane is used as the solvent and 1,1,2-$Mo_2(OAr)_3(NMe_2)_3$ when benzene is used as the solvent. Solution spectra are consistent with the presence of the gauche rotamer for 1,2-$Mo_2(OAr)_2(NMe_2)_4$, showing two types of NMe_2 groups, and the unique atom bond to each metal gauche to one another for 1,1,2-$Mo_2(OAr)_3(NMe_2)_3$, showing three types of NMe_2 groups. Variable-temperature ^1H NMR studies allow the activation energy for restricted rotation about the M-NMe_2 bonds to be estimated from coalescence temperatures while the use of spin-magnetization-transfer techniques has allowed more accurate measurements of the activation parameters for this process. Two-dimensional NMR has also been applied to probe possible rotation in these molecules about the Mo≡Mo bond.

Introduction

One of the most powerful uses of nuclear magnetic resonance spectroscopy is its application to the study of dynamic chemical processes.[1] In inorganic and organometallic chemistry this technique has allowed a number of exchange processes to be characterized that would otherwise not be amenable to study by other techniques. In particular, stereochemical nonrigidity and ligand fluxionality are important areas where it is possible to obtain relatively accurate kinetic measurements and such measurements have had an important impact on other aspects of chemistry in particular bonding ideas.

A series of molecules that exhibit a diverse and rich range of dynamic processes are early-transition-metal dinuclear complexes.[2] Here, dimer-monomer equilibria, bridge-terminal ligand exchange and, restricted (both electronic and steric) ligand mobility have been characterized in a number of systems.[3] Of particular interest

(1) Jackman, L. M.; Cotton, F. A. "Dynamic Nuclear Magnetic Resonance Spectroscopy"; Academic Press: New York, 1975.

(2) Cotton, F. A.; Walton, R. A. "Multiple Bonds Between Metal Atoms"; Wiley: New York, 1982.

0020-1669/85/1324-4565$01.50/0

to this present study are the dimetal systems M_2X_6 (M = Mo, W; X = R, NR_2, OR) first characterized by Chisholm and coworkers.[4,5] Here an unbridged, ethanelike geometry is typically adopted in which the six terminal ligands are arranged so that a staggered (D_{3d}) ground-state rotamer is formed. The metal–metal bonding for these complexes is then considered to involve overlap of predominantly metal d_{z^2}, d_{xz}, and d_{yz} atomic orbitals resulting in a $\sigma^2\pi^4$ triple bond for the M_2^{6+} core.[2,4] Three dynamic processes can be envisioned for these molecules: exchange of ligands between metals, rotation about the metal–metal bond, and possible restricted ligand mobility. In order to study such exchange, one normally has to synthesize heteroleptic molecules such as $M_2(X)_x(Y)_y$.[6-8] Evidence to date indicates that in the absence of added ligands, direct exchange of groups between metals is not facile. Electronically one would predict no barrier to rotation about the (M≡M) bond in these complexes, but the demonstration of this fact is not trivial. However, the use of sterically bulky ligands, especially dialkylamido groups, allows a sizeable rotation barrier to be imposed, resulting in the formation of anti and gauche rotamers for molecules of the type 1,2-$M_2X_2(NMe_2)_4$. Observation of the temperature dependence of the rate of exchange between rotamers of this type by NMR methods has allowed estimates of the steric barrier to rotation about the Mo≡Mo bond be made.[9,10]

Another interesting fluxional process involves dialkylamido ligands when bonded to these M_2^{6+} centers. The nitrogen-p to metal-d π-bonding that is a typical feature of early-transition-metal amido compounds involves donation to the metal d_{xy} and $d_{x^2-y^2}$ orbitals.[2,4] This partial double bond character to the M–NR_2 interaction hence imposes a preferred geometry for the ligand, with alkyl groups lying along the metal–metal axis. Hence for a $N(CH_3)_2$ ligand, one methyl group lies over the metal–metal bond (proximal) while the other lies away (distal). The diamagnetic anisotropy associated with the M≡M function results in a dramatic difference in the chemical shifts of the protons on these groups, typically over 2 ppm.[2] In the ^{1}H NMR spectrum, rotation about the M–NMe_2 bond is normally observed to be temperature dependent as seen by the broadening and collapse of the proximal and distal methyl group signals and their coalescence into a single resonance. Estimates of the value of ΔE for the rotational barrier have been made from the coalescence temperature for the exchange. Values obtained this way indicate barriers between 10 and 20 kcal mol^{-1}.[6] Another method for the determination of exchange rates of nuclei between nonequivalent sites involves the spin-magnetization-transfer technique.[11] This method has certain advantages and disadvantages over the more routine line-shape-analysis technique.[12] We wish to report here our initial exploration of this technique to the fluxionality problems associated with some (dialkylamido)dimolybdenum complexes.

Synthesis of Compounds

We have previously demonstrated that the reaction of $Mo_2(NMe_2)_6$ (Mo≡Mo) with phenolic reagents can lead to a range of products, depending on the steric demand of the ligand.[13] With the new ligand 2,6-diphenylphenol (HOAr-Ph_2) we have found that two substitution products can be obtained. In hexane solvent, addition of 2 equiv or more leads to a rapid and almost quantitative precipitate of 1,2-$Mo_2(OAr\text{-}Ph_2)_2(NMe_2)_4$ (**1**). In benzene or toluene solution (**1**) will react cleanly with another 1 equiv of HOAr-Ph_2 to give yellow solutions of 1,1,2-$Mo_2(OAr\text{-}Ph_2)_3(NMe_2)_3$ (**2**). Compound **2** can also be obtained from $Mo_2(NMe_2)_6$ and HOAr-Ph_2 (≥3 equiv) in benzene directly. Both compounds can be recrystallized from toluene on cooling.

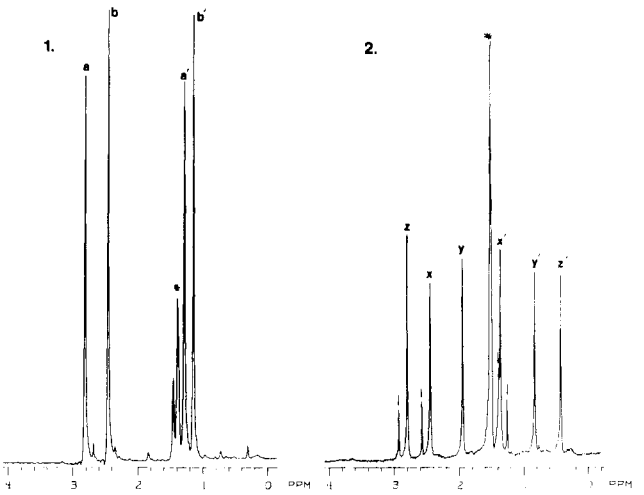

Figure 1. 200-MHz ^{1}H NMR spectra of the compounds $Mo_2(OAr\text{-}Ph_2)_2(NMe_2)_4$ (**1**) and $Mo_2(OAr\text{-}Ph_2)_3(NMe_2)_3$ (**2**) at 10 °C (**1**) and −10 °C (**2**) in toluene-d_8. A small amount of **1** as a contaminant of **2** is indicated by arrows, while the protio impurities in toluene-d_8 are indicated by an asterisk.

Solution Structure and Fluxionality of 1 and 2

The low-temperature (10 °C) ^{1}H NMR spectrum of (**1**) (Figure 1) is consistent with the adoption of the gauche rotamer in solution, with no signals identifiable with the anti rotamer being observed. The qualitative appearance of this spectrum is somewhat similar to that of 1,2-$Mo_2(OAr')_2(NMe_2)_4$ (OAr' = 2-*tert*-butyl-6-methylphenoxide), which has been shown to adopt a gauche rotamer in the solid state.[13a] In the aliphatic region of the spectrum of (**1**) four different N–CH_3 resonances can be seen. These correspond to the proximal (low field) and distal (higher field) methyl protons of the two different NMe_2 groups of the gauche rotamer. From the sharp, well-resolved nature of these signals, one can conclude that rotation about both the Mo—N and Mo≡Mo bonds is slow on the NMR time scale at this temperature. Attempts to assign the two types of NMe_2 groups with the observed pairs of resonances cannot be made. When solutions containing (**1**) are warmed up, both sets of proximal (a,b) and distal (a′, b′) methyl group resonances begin to broaden and coalescence toward each other. From the coalescence temperatures, one can obtain an estimate on the barrier to rotation about the Mo–NMe_2 bonds as 15.8 ± 0.5 (a) and 16.6 ± 0.5 (b) kcal mol^{-1}. However, an assumption implicit in this treatment is that rotation about the Mo≡Mo bond is not significant over the temperature range of the experiment.[9] Such a rotation would have the effect of exchanging sites a with b and a′ with b′. Hence, at high temperatures one would predict all methyl resonances to collapse into a single peak, whereas restricted rotation about Mo≡Mo would give rise to two separate peaks at the average position of peaks a, a′ and b, b′. Unfortunately, we have not obtained high-temperature limiting spectra. At the highest temperatures used (85 °C) the methyl signals appeared as one broad resonance. In order to answer this question we carried out a two-dimensional-exchange ^{1}H NMR experiment at 38 °C (Figure 2). As can be seen, proximal–distal exchange of peaks a–a′ and b–b′ is rapid at this temperature while rotation about the metal–metal bond, peaks a–b and a′–b′, is extremely slow as shown by the cross peak contours.

In order to gain more accurate activational data for these processes under more ambient temperature conditions, we have investigated the use of Forsên–Hoffmann spin saturation exchange

(3) Chisholm, M. H.; Rothwell, I. P. *Prog. Inorg. Chem.* **1982**, *29*, 1.
(4) Chisholm, M. H.; Cotton, F. A. *Acc. Chem. Res.* **1978**, *11*, 336.
(5) Chisholm, M. H. *Polyhedron* **1983**, *2*, 681.
(6) Chisholm, M. H.; Huffman, J. C.; Rothwell, I. P. *Organometallics* **1982**, *1*, 251.
(7) Chisholm, M. H.; Folting, K.; Haitko, D. A.; Huffman, J. C. *J. Am. Chem. Soc.* **1981**, *103*, 4046.
(8) Chisholm, M. H. *Symp. Faraday Soc.* **1980**, *14*, 194.
(9) Chisholm, M. H.; Rothwell, I. P. *J. Am. Chem. Soc.* **1980**, *102*, 5950.
(10) Chisholm, M. H.; Rothwell, I. P. *J. Chem. Soc. Chem. Comm.* **1980**, 985.
(11) Forsên, S.; Hoffmann, R. A. *J. Chem. Phys.* **1963**, *39*, 2892.
(12) Forsên, S.; Hoffmann, R. A. *J. Chem. Phys.* **1964**, *40*, 1189.
(13) (a) Coffindaffer, T. W.; Rothwell, I. P.; Huffman, J. C. *Inorg. Chem.* 1985, 24, 1643. (b) Coffindaffer, T. W.; Rothwell, I. P.; Huffman, J. C. *Inorg. Chem.* **1984**, *23*, 1433. (c) Coffindaffer, T. W.; Rothwell, I. P.; Huffman, J. C. *Inorg. Chem.* **1983**, *22*, 2906. (d) Coffindaffer, T. W.; Niccolai, G.; Powell, D.; Rothwell, I. P.; Huffman, J. C. *J. Am. Chem. Soc.* **1985**, *107*, 3572.

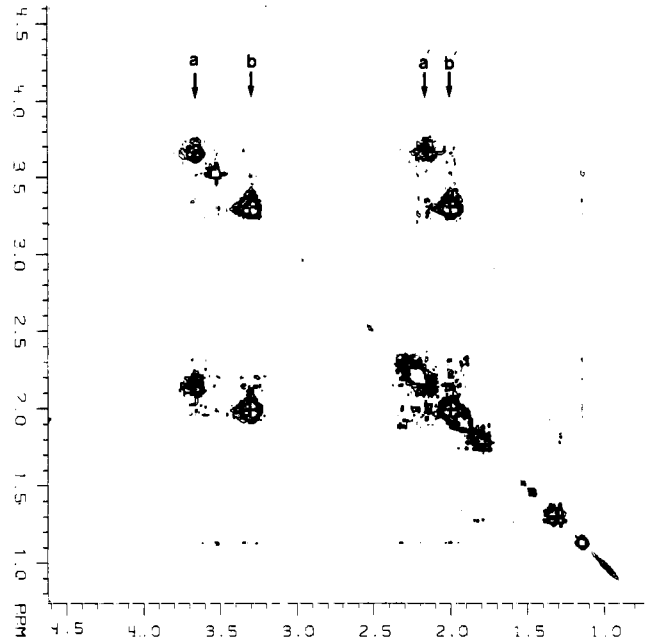

Figure 2. Two-dimensional ^1H NMR of complex $Mo_2(OAr\text{-}Ph_2)_2(NMe_2)_4$ (**1**) at 38 °C showing exchange of proximal–distal methyl groups (peaks a–a′, b–b′) but negligible exchange of nonequivalent amido ligands, (peaks a–b, a–b′, b–a′, or a′–b′).

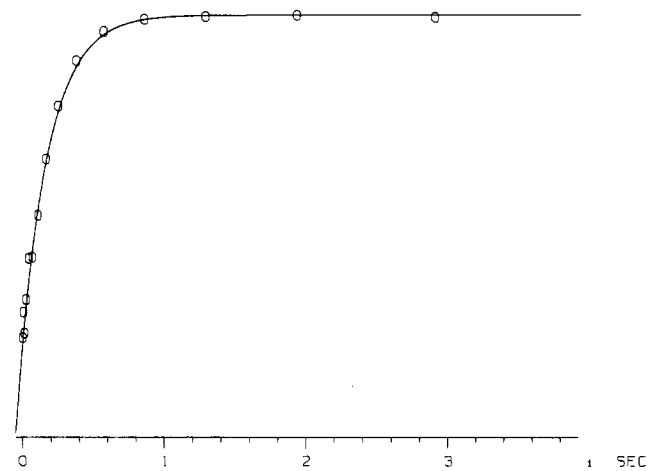

Figure 3. Recovery of the intensity of methyl group resonance b of $Mo_2(OAr\text{-}Ph_2)_2(NMe_2)_4$ (**1**) at 16 °C after a 180° pulse. Methyl group resonance b′ is being irradiated throughout.

experiments.[11,12] In particular the recovery of the proximal NMR signal intensities on removal of a saturating rf field centered on the exchanging distal partners (Figure 3). From these data the longitudinal relaxation time was measured.[14,15] The rate constant of exchange was then obtained from the value of the longitudinal relaxation time, the intensity of the observed peak while the exchanging partner is saturated, and the intensity of the peak with off-resonance irradiation. Rate data for both sets of Mo–NMe_2 groups were obtained at five temperatures between 10 and 35 °C and are collected in the Experimental Section. The use of Arrhenius and activated complex theories (Figure 4) allowed the activation parameters given in Table I to be obtained. It can be seen that the data gives values of E_a close to the value of $\Delta G^{\ddagger}$ calculated from T_c data, while the entropy of activation for the process is small as one would expect for a bond rotation process.

For complex (**2**) there is again the possibility of two rotameric forms in solution. As shown by Newmann projections (Chart I)

(14) Levitt, M. H.; Freeman, R. *J. Magn. Reson.* **1979**, *33*, 473.
(15) Freeman, R.; Kempsel, S. P.; Levitt, M. H. *J. Magn. Reson.* **1980**, *38*, 453.

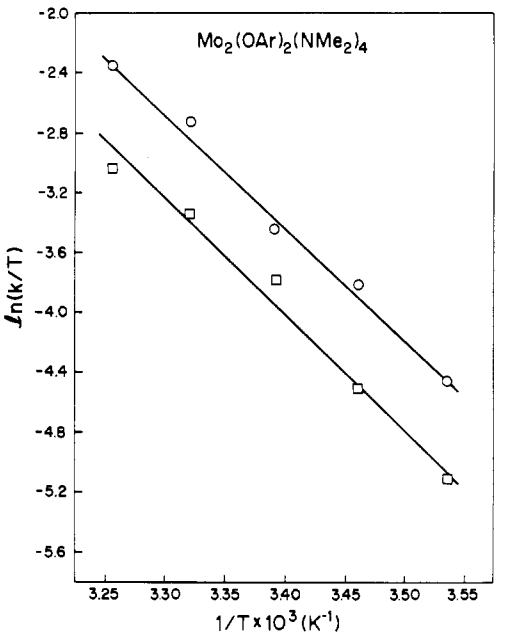

Figure 4. Activated complex theory plot for the exchange of the methyl groups (peaks a–a′ and b–b′) in $Mo_2(OAr\text{-}Ph_2)_2(NMe_2)_4$ (**1**).

Table I. Activation Parameters for Rotation about the Mo–NMe_2 Bonds in $Mo_2(OAr\text{-}Ph_2)_2(NMe_2)_4$ (**1**) and $Mo_2(OAr\text{-}Ph_2)_3(NMe_2)_3$ (**2**)[a]

	1		**2**	
NMe_2 peak	a	b	x	y
$\Delta G^{\ddagger}$ (T_c)	15.8 ± 0.5 (72)	16.6 ± 0.5 (85)	15.6 ± 0.5 (62)	15.1 ± 0.5 (52)
E_a	15.7 ± 0.5	15.9 ± 0.5	16.9 ± 0.5	17.0 ± 0.5
log A	12.6 ± 1.5	12.5 ± 1.5	14.0 ± 2	14 ± 2
$\Delta H^{\ddagger}$	15.1 ± 0.5	15.3 ± 0.5	16.4 ± 0.5	16.4 ± 0.5
$\Delta S^{\ddagger}$	−3 ± 4	−3 ± 4	+4 ± 4	+3 ± 4

[a] $\Delta G^{\ddagger}$, E_a, and $\Delta H^{\ddagger}$ in kcal mol^{-1}, $\Delta S^{\ddagger}$ in entropy units, and T_c in °C.

Chart I

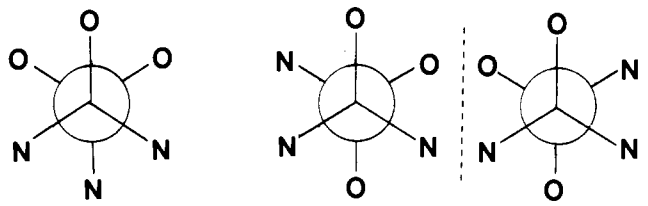

(I) **(II)**

rotamer I would be expected to have two types of NMe_2 groups in the ratio of 2:1 while in II and its enantiomer all three NMe_2 functions are nonequivalent. The low-temperature spectrum of **2** (Figure 1), showing six sharp, nonequivalent N–CH_3 resonances, three proximal and three distal, is hence consistent with the presence in solution of rotamer II in which proximal–distal exchange is slow. When solutions of **2** are warmed, proximal–distal exchange occurs for the resonances of two of the three types of NMe_2 groups, peaks x–x′ and y–y′. However, exchange of the other methyl resonances, peaks z–z′, does not begin on the NMR time scale until above 130 °C (90 MHz). From the coalescence temperatures we can estimate the activation energies as 15.6 ± 0.5 (peak x) and 15.1 ± 0.5 (peak y) kcal mol^{-1} for the more fluxional groups while the barrier to rotation of the group denoted by peak z can only be estimated as above 21 kcal mol^{-1} due to the temperature limitations of the instrument. This latter figure represents the highest barrier to proximal–distal exchange yet reported, and we believe this NMe_2 group to be the one coordinated to the Mo atom containing two OAr-Ph_2 ligands. Hence

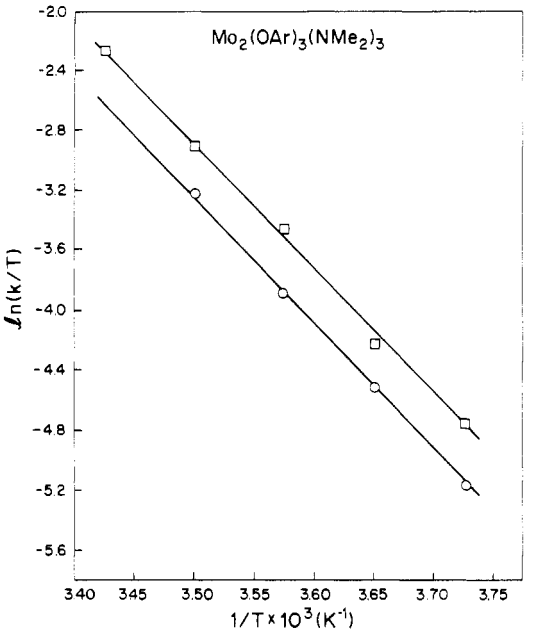

Figure 5. Activated complex theory plot for the exchange of the methyl groups (peaks x–x′ and y–y′) in $Mo_2(OAr\text{-}Ph_2)_3(NMe_2)_3$ (**2**).

the unusually high barrier to rotation probably reflects the presence of the two very bulky aryloxide groups sterically hindering the ligand rotation. The other two NMe_2 groups are in environments similar to that found in compound (**1**) and the similarity of the values of $\Delta G^{\ddagger}$ is consistent with this.

We have also applied the Forsén–Hoffmann technique to study the exchange of the NMe_2 groups giving resonances x and y in complex **2** (Figure 5). Activational parameters are collected in Table I. Again the data are consistent with those obtained from the coalescence temperature, but this time the entropy of activation is slightly positive, compared to a slightly negative value found for complex **1**. Presumably, the values represent small changes in degrees of freedom of motion of the other ligation in the molecule on going to the transition state. However, further attempted interpretation of such small changes in $\Delta S^{\ddagger}$ would be foolish, especially in view of the relatively large errors involved in these measurements.

Conclusions

The use of spin-magnetization transfer appears to be a good method for the investigation of restricted bond rotation in dialkylamido complexes of this type. In particular the method would be of great use for systems that are thermally sensitive, thus not allowing coalescence temperatures to be measured. The two-dimensional NMR experiment indicates that although Mo–NMe_2 bond rotation is facile, rotation about the Mo–Mo triple bond is negligible in these particular compounds.

Experimental Section

Proton nuclear magnetic resonance spectra were obtained on a Nicolet NT-200 spectrometer operating at 200.068 MHz. The spectral width was 2020 Hz, and the free induction decays were detected in quadrature, digitized into a 12 bit ADC, and collected into 4096 data points. The resulting digital resolution was 0.5 Hz. The temperature of the sample was maintained at ±1 °C with the variable-temperature unit, which had previously been calibrated by using an acidified methanol solution.[16] The exchange rates were measured with the method of Mann.[17] The longitudinal relaxation time was measured by using the inversion recovery method containing a composite 180° pulse[14,15] while the exchanging partner was irradiated with the homonuclear decoupler during all but the acquisition time. The relaxation time was obtained from a three-parameter fit.[18] The rate of exchange is obtained from the values of the longitudinal relaxation time, the intensity of the observed peak while the exchanging partner is saturated, and the intensity of the peak with off-resonance irradiation.

The 2D-exchange NMR spectrum was obtained as previously described[19] except without the use of the magnetic field gradient pulse. The axial peaks and transverse components were eliminated by inverting the phase of the first and third pulses of every acquisition.[20] The parameters used during acquisition were as follows: relaxation delay, 1.5; sweep width in both dimensions, 776.447; mixing time, 1 s, acquisition time, 330 ms.

Preparation of 1,2-$Mo_2(OAr\text{-}Ph_2)_2(NMe_2)_4$ (1). To a solution of $Mo_2(NMe_2)_6$ (0.40 g, 0.90 mmol) in hexane (30 mL) was added 2,6-diphenylphenol ($HOAr\text{-}Ph_2$; 0.47 g, 1.90 mmol). The solution was allowed to stir at room temperature, resulting in a yellow precipitate. The yellow solid was filtered off and dried under vacuum. Recrystallization by slow diffusion of hexane through a saturated toluene solution of the yellow solid yielded the yellow crystalline solid $Mo_2(OAr\text{-}Ph_2)_2(NMe_2)_4$ in good yield. Anal. Calcd for $Mo_2C_{44}H_{50}N_4O_2$: C, 61.54; H, 5.87; N, 6.52. Found: C, 62.20; H, 6.09; N, 6.59. ^1H NMR (toluene-d_8, 10 °C): δ 6.80–8.10 (m, $OC_6H_3(C_6H_5)_2$), 3.59 (s, NMe_2^a), 3.26 (s, NMe_2^b), 2.12 (s, $NMe_2^{a'}$), 1.96 (s, $NMe_2^{b'}$).

Preparation of 1,1,2-$Mo_2(OAr\text{-}Ph_2)_3(NMe_2)_3$ (2). To a solution of $Mo_2(NMe_2)_6$ (0.50 g, 1.10 mmol) in benzene (30 mL) was added 2,6-diphenylphenol ($HOAr\text{-}Ph_2$; 1.10 g, 4.40 mmol). The mixture was allowed to stir at room temperature for 7 h; evaporation of benzene yielded a yellow solid. Recrystallization by slow diffusion of hexane through a saturated toluene solution of the yellow solid yielded the yellow crystalline solid $Mo_2(OAr\text{-}Ph_2)_3(NMe_2)_3$ in good yield. Anal. Calcd for $Mo_2C_{60}H_{57}N_3O_3$: C, 67.98; H, 5.42; N, 3.96. Found: C, 67.95; H, 5.35; N, 3.58. ^1H NMR (toluene-d_8, −15 °C): δ 6.8–8.1 (m, $OC_6H_3(C_6H_5)_2$), 3.49 (s, NMe_2^z), 3.13 (s, NMe_2^x), 2.63 (s, NMe_2^y), 2.04 (s, $NMe_2^{x'}$), 1.52 (s, $NMe_2^{y'}$), 1.13 (s, $NMe_2^{z'}$).

Acknowledgment. We thank the National Science Foundation (Grant CHE-8219206 to I.P.R.) for support of this work. T.W.C. gratefully acknowledges receipt of an Amoco Fellowship. We thank Purdue University Biochemical Magnetic Resonance Laboratory supported by NIH Grant RR01077 from the Biotechnology Resource Program of the Division of Research Resources.

Registry No. **1**, 99248-75-6; **2**, 99248-76-7; $Mo_2(NMe_2)_6$, 51956-20-8; Mo, 7439-98-7.

Supplementary Material Available: Tables of the intensity measurements, T_1's, and exchange rates at various temperatures for the proximal methyl groups (peaks a, b, x, and y) (2 pages). Ordering information is given on any current masthead page.

(16) van Geet, A. L. *Anal. Chem.* **1970**, *42*, 679.
(17) Mann, B. E. *J. Magn. Reson.* **1977**, *25*, 91.
(18) Levy, G.; Peat, *J. Magn. Reson.* **1975**, *18*, 500.
(19) Jeener, J.; Meier, B. H.; Bachmann, P.; Ernst, R. R. *J. Chem. Phys.* **1979**, *71*, 4546.
(20) Macura, S.; Ernst, R. R. *Mol. Phys.* **1980**, *41*, 95.